

HIGH FREQUENCY MEASUREMENTS OF CURRENT THROUGH INDIVIDUAL ANODES: SOME RESULTS FROM MEASUREMENT CAMPAIGNS AT HYDRO

Steinar Kolås¹, Phillip McIntosh¹, and Asbjørn Solheim²

¹ Hydro Primary Metal Technology; P.O. Box 303, NO-6882 Øvre Årdal, Norway

² SINTEF Materials and Chemistry; P.O. Box 4760 Sluppen, NO-7465 Trondheim, Norway

Keywords: Anode, Current Distribution, Current Pickup, Anode Effect

Abstract

Long term measurement campaigns were conducted at Hydro Aluminium's Reference Centre in Årdal. The work comprised high frequency measurements of all individual anode current loads in three test cells. Typical patterns of current load as a function of the anode age are presented and discussed. Middle-aged anodes showed increased current fluctuations, which could be related to the anode setting pattern. The current load started increasing when the anode slots had worn away. This is apparently explained by a decreasing anode-cathode distance. It was possible to provoke local anode effects (AE) at one or more individual anodes by manipulation of the alumina feeders. Such AEs were detected as sudden drops in the current without significant increase in the cell voltage. All observed general AEs were initiated on old anodes where the slots had worn away.

Introduction

Traditionally, the amperage and the cell voltage are the only parameters being measured continuously in aluminium reduction cells. It would be beneficial to introduce more measurements to improve the cell control, and the idea of metering the current through individual anodes is neither new nor original. Such measurements have been described in several papers [1-5]. Still, very few plants have cells equipped with devices for continuous logging of the current distribution on a standard basis. Such measurements generate huge amounts of data, and – arguably – only recently, the increasing speed and storage capacity of computers have made such data acquisition and handling practicable.

There are several reasons why the anodic current distribution is interesting. Early detection of anodes that have been set too high or too low and location of anode spikes and deformations are obvious advantages. It may also be possible to detect faulty alumina feeders. Furthermore, the current efficiency (CE) depends, among other things, on the anode-cathode distance (ACD), in such a way that the CE decreases sharply when the ACD is lower than a certain critical limit [6]. Therefore, acceptable CE at low average ACD requires uniform ACD [2, 4], and knowledge of the current distribution may be the basis for corrective actions. Furthermore, it has been observed that the individual current loads start diverging as the cell becomes starved in alumina [1]. Although the increase in the total cell voltage also can be used as an anode effect (AE) warning [5], the AE always starts at an individual anode, and knowledge of the current distribution could be the basis for an earlier warning. Local

alumina starvation would be detected earlier, and it may be feasible to increase the alumina feeding only in the critical part of the cell.

Local alumina starvation also seems to be related to the observation of a positive baseline of perfluorocarbon (PFC) compounds [5, 7]; *i.e.*, there are local AEs that are not accompanied by abruptly increasing cell voltage. Most aluminium companies make use of an instrumental definition of the AE; *i.e.* the AE is defined as a period with cell voltage above a certain value. However, local AEs can only be discovered by PFC measurements or by metering of the anodic current distribution, as discussed in the present paper.

The main motivation for the measurement campaigns was to learn more about the relationship between anodic current distribution and alumina feeding, with a special view to the redistribution of current following local variations in the alumina concentration and the setting of new anodes. A comprehensive analysis of the data is not yet completed. The present paper is focused on the current pickup as a function of time and the onset of the anode effect.

Experimental

Location

The measurements were performed at Årdal Reference Centre. Two types of cells were studied; HAL4e (426 kA, 40 anodes; see the description by Bardal *et al.* [8]) and HAL300 (318 kA, 30 anodes). In the HAL4e cell the test lasted for more than three full anode cycles, while it lasted for approximately fourteen full anode cycles in the HAL300 cells. All cells had anode setting patterns based mainly on double change of anodes.

Electrical Measurements

The currents were measured by recording the voltage drop along 10 cm of the anode stem or current riser. The measurements comprised 40 (30) anode stems, the current risers, and the total cell voltage. In addition, the temperature was recorded at the risers and at 10 anode stems, and temperature corrections were made by means of a stem temperature model that evolved during the project. In HAL300, bath sensing signals were also collected by recording the voltage drop between the breaker of the alumina point feeder and the cathode. The data acquisition system was based on a QuantumX logger and a Getac PC with flash disc and appropriate software. The logging frequency varied from 1Hz to 19kHz, and during the project, about 2 Terra Bytes of data was generated.

Current Pickup

Measurements and Model

To help analysing and interpreting the data, a simple anode model was programmed in an Excel spreadsheet. The main features of the model are illustrated in Figure 1. A constant voltage of 2.6 V. was applied between the anode beam and the metal pool; this corresponds approximately to the total cell voltage reduced by the external voltage drop, the cathode voltage drop, and the reversible cell voltage. The anodic overvoltage was calculated by a semi-empirical equation given by Grjotheim and Kvande [9], and the electric conductivity of the bath was taken to be $212 \text{ ohm}^{-1}\text{m}^{-1}$ as calculated by the equation of Hives *et al.* [10] for a bath containing 11.5 wt% excess AlF_3 , 5 wt% CaF_2 , and 3.5 wt% Al_2O_3 . The ohmic resistance of the carbon (R_c) was estimated as a function of the remaining height and the reduction of the cross sectional area due to airburn (counted as a linear reduction of the horizontal anode dimensions). The extra ohmic voltage drop due to the presence of gas bubbles ("bubble overvoltage") was assumed to be proportional with the ratio between the base area and the periphery length of the working surface(s) of the anode; implying that the bubble voltage drop increases by a factor of approximately 2.5 as the slots wear away. Corrections were also made for the Boudouard reaction and dusting (assumed to take place at the submerged part of the anode, including the slots).

Figure 2 shows the average current pickup for the 30 anode positions in the HAL300 cell as a function of the anode age. The modelled current pickup is shown in the same figure. Figure 3 shows the modelled ACD. As can be observed, the simple model was able to capture the main features of the current pickup course. For convenience, the lifetime of the anode was divided into four periods, which will be discussed in terms of the measurements and the model in the following.

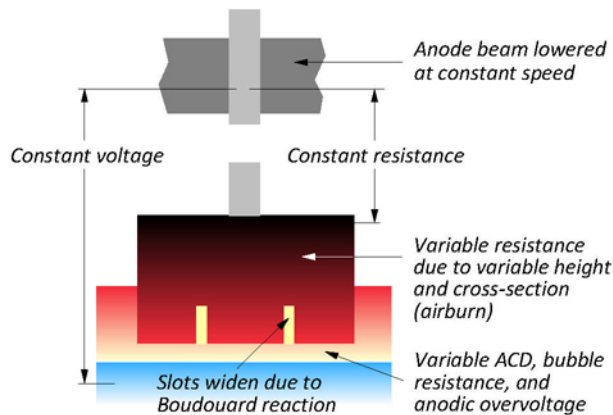


Figure 1. The main features of a spreadsheet model for calculating the current pickup.

Period I: The Young Anode

The first five days after setting of a new anode were not modelled. Still, some general comments can be made.

A newly set anode is cold, and a freeze will be formed that extends all the way down to the metal. The setting of a new anode (normally two at a time) therefore represents a serious disturbance

of the cell. This goes for the redistribution of current, the alumina consumption pattern, and also the bath flow pattern, because more than 40 percent of the electrolyte cross-sectional area will be blocked by frozen bath.

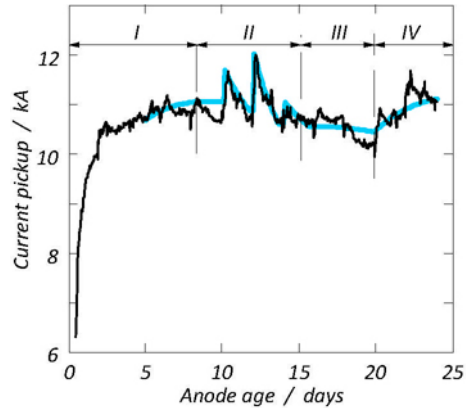


Figure 2. Thin black curve – measured current pickup as a function of the anode age (average of 30 anodes in a HAL300 cell), thick blue curve – calculated current pickup. The anode lifetime is divided into four periods.

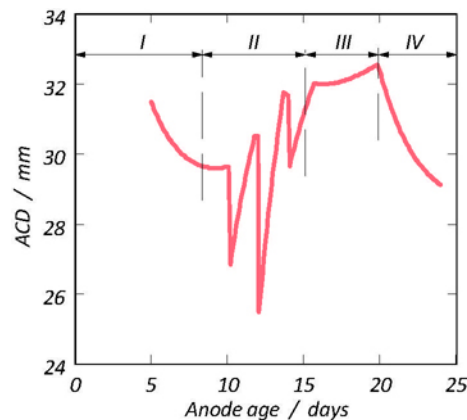


Figure 3. Calculated anode-cathode distance as a function of the anode age (same calculation as shown in Figure 2).

Ødegård *et al.* [11] carried out experiments in an industrial cell, and they found that the freeze melted away after about 10 hours. An anode that was taken out 90 minutes after setting was completely covered by freeze at the underside, but no freeze was found at the sides. An explanation for this was later offered by Thonstad [12]; freshly formed freeze is pushed off the sides due to de-gassing of the anode during heat-up (the anode contains about 25-30 percent pores).

The data for the HAL300 cell indicated that the current increases almost linearly up to 80 percent of the average current after 16 hours, followed by a new linear increase with lower slope up to 97 percent of the average current after 48 hours. It is likely that double-shifting of anodes gives longer re-melting time than reported by Ødegård *et al.* [11], since one side of the anode will be

facing an equally cold neighbouring anode. It can, therefore, be suggested that the course during the first 16 hours represents the re-melting period.

The new anode is normally set 25 mm higher than the removed anode, leading to an ACD that is somewhat higher than average after the re-melting period. The current increase after 16 hours is probably mainly related to decreasing ACD (see Figure 3), but also, the anode is being further heated, giving tighter contact between the carbon and the cast iron used in the stub hole.

Period II: Midlife Crisis

The middle-aged anodes are the ones that carry the highest current, as shown in Figure 2. The current pickup varies a lot when the anode is between 10 and 14 days old.

Double anode shifts in a cell with 30 anodes gives 7.1 percent average current increase through the working anodes in the re-melt period, corresponding to 0.75 kA in the present case. Such large variations can generally not be observed in Figure 2, probably because the effect of setting will be partly smeared out when the anodes are not set at the exact same time of day. It has been observed that the setting of a new anode mainly affects the neighbouring anodes. It appears that the large variations at ages between 10 and 14 days can be related to the anode setting pattern in this specific cell, since all the neighbouring anodes were set in this time span, as illustrated in Figure 4.

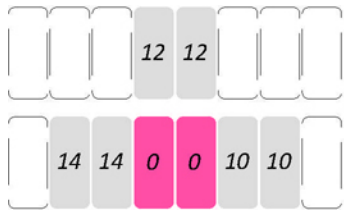


Figure 4. Anode setting pattern in the HAL300 cell studied. Neighbouring anodes in the same row are always set 10 and 14 days after setting of the anodes marked "0", while the neighbours "across the street" are set after 12 days.

It is well known that the current through the cell leads to electromagnetically induced compressive forces on the body of the metal, distorting the metal in such a way that the level may be several cm higher at the middle of the cell than at the corners. When an anode is changed, this force decreases locally, leading to a redistribution of the metal surface level. The recorded current pickup data could be approximately reproduced in the model by introducing sudden increases in the local metal level ranging from 2 to 5 mm when the neighbouring anodes are changed followed by a linear restoration of the metal level (see Figure 3). The modelled current is shown in Figure 2. It appeared that setting of anodes "across the street" had the largest influence.

Another explanation for the local change in metal height is possible. It was derived earlier that the local metal level depends on the local alumina concentration, due to the variation in the density of the bath [2, 4]. It is, therefore, possible that the variation in the metal level is caused by changes in the alumina distribution following the new patterns of bath flow and alumina consumption.

Period III: Decreasing Performance

Anodes older than about 15 days start to lose current. This might be somewhat surprising since the anode slots are still active; the anode stud-carbon contact is normally very good at this stage, and the resistance in the carbon is lower because around 50 percent of the original anode height has worn away in this period. However, also the cross-sectional area of the anode is important, and this will be lower than average in this period. The slots are still present, and at the time of setting, about 4.2 percent of the nominal working area is slots. This number increases with time because the slots expand somewhat due to the Boudouard reaction and because there will be a small current also inside the slot. Furthermore, the horizontal dimensions decrease due to airburn at the sides. Besides the effect of the smaller active working area *per se*, the anode will wear away more rapidly than the motion of the anode beam, resulting in a slightly increasing ACD as shown in Figure 3.

Period IV: Indian Summer

The sharp current increase at 20 days age coincides with the time when the slots in the anode are worn away. This gives increased "bubble overvoltage", which would be expected to contribute to further reduction of the current. However, it appears that the effect of increased active area, which was mentioned in the previous section, dominates. Taking into account the widening of the slots and the shrinking horizontal anode dimensions due to airburn, the working area may increase as much as 10 percent when the slots disappear. This gives smaller resistance as well as a correspondingly lower linear wear rate. The anode beam is lowered at a constant rate, and the resulting decrease in ACD is shown in Figure 3.

The current pickup in HAL4e followed a similar pattern as described above provided that the anode change cycle was the same. Increased current fluctuation on mid-aged anodes was not observed however, since this cell had a different anode setting pattern. The time scale was also somewhat different, due to different anode heights and slot depths.

Concepts for Data Visualisation and Analysis

While measuring the current in 30/40 anodes simultaneously is a challenge in itself, analysing the large amount of data is another challenge. The straight forward concept would be to look at the anode current measurements only, as discussed in the previous chapters or as seen in Figure 5 below. However, in order to gain more knowledge, different concepts for visualisation and analysis were developed.

In order to understand the measured current data it was important to relate it to other information from the cells. One concept chosen was to combine the measured data with knowledge regarding the anode setting pattern and the current state of each individual anode. Hence, the knowledge of the current pickup in the anodes could be developed to a level beyond interpreting the current data only. An example is shown in Figure 6 below, where anodes are grouped around each feeder and where the current pickup is analysed according to anode setting patterns and anode age.

In Figure 6, the dark blue colour indicates an area with newly set anodes with low current pickup. Red means an area with anodes with high current pickup. Figure 6 shows that at an anode change,

the current is systematically redistributed to other areas given by the anode setting pattern.

Another strategy chosen was to combine the measured data with knowledge regarding the anode setting pattern with respect to remaining slot height and remaining anode height, by utilizing “videos” to get an increased understanding of what was going on in the cell. A snapshot of this concept is shown in Figure 7, which illustrates that a partial AE is emerging on anode 37 and 38 as well as that the slots on these anodes is consumed. Further, it was possible to use this technique to detect which anodes that was following anode 37 and 38 towards the full AE.

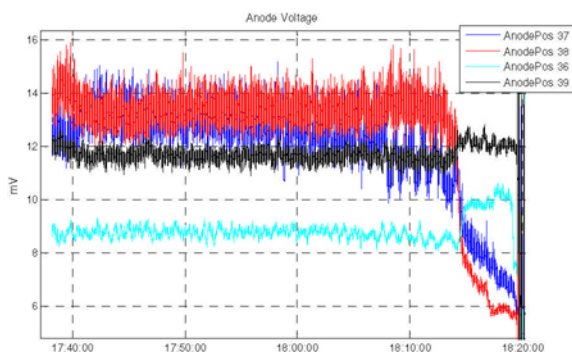


Figure 5. The figure shows the current measurements on four anodes, where two anodes (red and blue) go into partial AE approximately 5 minutes before the general AE (at the end of the figure).

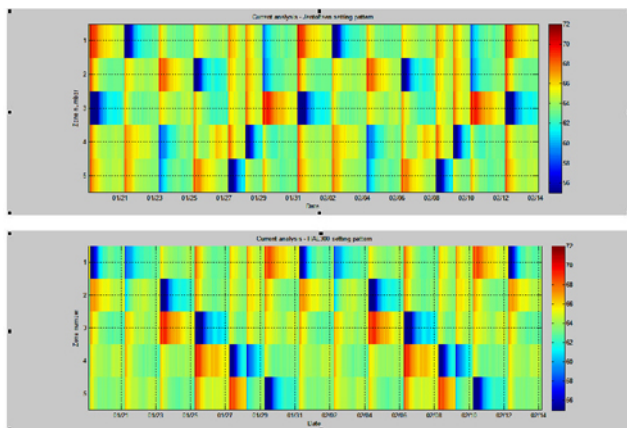


Figure 6. Patchwork concept: The figure shows how the current pickup in a group of anodes changes based on anode setting patterns and current pickup as a function of anode age. Data obtained by with two different anode setting patterns.

Anode Effect

Partial Anode Effect

A number of AEs were observed during the periods of measurement. These AEs occurred either “naturally” or were provoked by redistributing the alumina feeding locally in the cell. It was found that the AE always started with partial anode effects, *i.e.* the current dropped low at one or two anodes, as shown in Figure 5 above.

The AE can be defined as PFC generation due to increased anode voltage (sum of reversible voltage and anodic overvoltage). The onset of an AE has often been described as a kind of domino effect; the AE starts at the anode that “sees” the lowest alumina concentration, and the current is re-distributed to the other anodes causing the next anode to develop AE, *etc.* Provided that the alumina distribution is non-uniform; the AE at the first one or two anodes will not spread to the rest of the cell, simply because the other anodes have ample supply of alumina. During a partial AE, the voltage drop between the anode beam and the metal will be re-distributed from the ohmic terms to the anode voltage. As explained by Thonstad *et al.* [13] this voltage drop between the anode beam and the metal is more than high enough to sustain the AE. The partial (or “local”) AE should not be termed “non-AE PFC generation”.

The partial AEs were not accompanied by a significant rise in the cell voltage, and they were not recorded as AE by the process control system. In one case, such a partial AE was quenched by adding a few hundred grams of alumina, which illustrates the potential of individual anode current measurements for early warning of AE.

A mechanism behind the off-and-on current pattern during partial AE is suggested in the following,

1. During normal electrolysis, alumina is consumed at the anode. Alumina must be transported to the anode by diffusion through a boundary layer close to the anode. The concentration difference between the bulk and the anode is in the order of 1 wt% Al_2O_3 .
2. When the alumina concentration at the anode falls to very low values, the anode voltage starts increasing. The current and the ohmic voltage decrease, while the total voltage drop between the anode and the metal stays constant. Eventually, the anode voltage becomes high enough to produce PFC.
3. The PFC (or the very low alumina concentration) leads to a very low wetting angle the bath and the carbon. Consequently, a gas film is formed at the underside of the anode, and the current falls to a very low value.
4. During the period with low current there is no consumption of alumina, and the alumina concentration at the anode surface increases until the concentration is high enough to quench the AE.
5. Since the alumina concentration in the bulk is not sufficient to sustain normal electrolysis, steps 2-4 will be repeated.

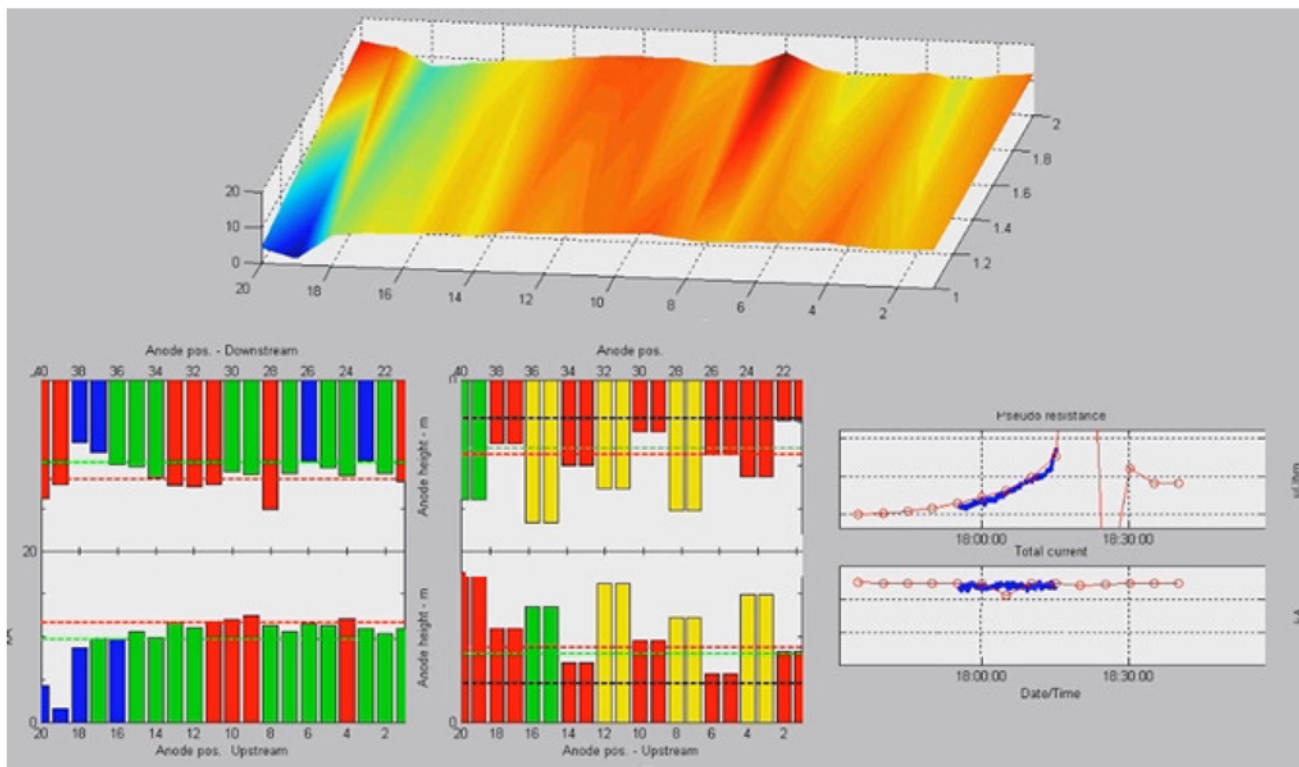


Figure 7. The figure shows the current pickup in each anode (left bar graph and 3D figure), the level for when the slots are consumed (red and green dotted lines in right bar graph), the remaining height of the anode in each position in the cell (bars in right bar graph), and the pseudo resistance and current (time plots, right hand side).

Anode Effect and Slots

It was observed that partial AEs, and also the initiation of general AE, with very few exceptions started at the oldest anode pair – or at least, at old anodes where the slots had worn away. To the authors' best knowledge, this has not been reported in the literature earlier. There may be several reasons for this, and some possible explanations are listed below.

- Old anodes generally carry much current, because they develop low ACD (Figs. 2 and 3). Also, part of the sides is worn away due to airburn and the Boudouard reaction, leading to a smaller cross-sectional area. This means that the current density will be higher than at the average anode.
- High current requires a larger alumina supply rate, while the small ACD gives a narrower path for alumina transport. Provided that the pressure distribution underneath the anode is constant, the linear velocity is approximately independent of the ACD, and the bath exchange rate underneath the anode ($\text{kg}\cdot\text{s}^{-1}$) becomes inversely proportional with the ACD.
- Anodes without slots probably have larger bubbles, longer bubble travelling distance along the working surface, and larger area fraction covered by bubbles. As a result, the "real" current density (between the bubbles) will be larger.

Concluding Remarks

High frequency measurements of current through individual anodes have proven to give useful information and insight concerning the conditions of the electrolysis cell. Obviously, spikes and wrongly set anodes are easily detected. Also, the redistribution of the current at anode change related to the anode setting pattern can be accounted for by automatically redistributing the alumina feeding accordingly. Further, partial AE is easily discovered and can be utilized by the pot process control system to bring any technology towards zero AE as well as minimizing PFC to the environment.

Acknowledgement

The present work was financed by the HAL UP Fundamentals programme, funded by the Research Council of Norway and Hydro Aluminium. Permission to publish the results is gratefully acknowledged.

References

1. K.Å. Rye, M. Königsson, and I. Solberg, "Current Redistribution among Individual Anode Carbons in a Hall-Heroult Prebake Cell at Low Alumina Concentration", Light Metals 1998, pp. 241/46.

2. A. Solheim and B.P. Moxnes, "Anodic Current Distribution in Aluminium Electrolysis Cells," paper presented at the XIII International Conference "Aluminium of Siberia-2007", Krasnoyarsk, Russia, 11-13 September, 2007 (Proceedings, pp. 21/27).
3. J. Keniry and E.P. Shaydulin, "Anode Signal Analysis – the Next Generation in Reduction Cell Control", paper presented at the XIII International Conference "Aluminium of Siberia-2007", Krasnoyarsk, Russia, 11-13 September, 2007 (Proceedings, pp. 4/11).
4. B. Moxnes, A. Solheim, M. Liane, and A. Halkjelsvik, "Improved Cell Operation by Redistribution of the Alumina Feeding", Light Metals 2009, pp. 461/66.
5. Abdalla Al Zarouni and Ali Al Zarouni, "DUBAL's Experience of Low Voltage PFC Emissions", paper presented at the 10th Australasian Aluminium Smelting Technology Conference, 9-14 October, 2011, Launceston, Tasmania.
6. S. Rolseth, T. Muftuoglu, A. Solheim, and J. Thonstad, "Current Efficiency at Short Anode-Cathode Distance in Aluminium Electrolysis", Light Metals 1986, pp. 517/23.
7. W. Li, X. Chen, J. Yang, C. Hu, Y. Liu, D. Li, and H. Guo, "Latest Results from PFC Investigation in China", Light Metals 2012, pp. 619/22.
8. A. Bardal, B.E. Aga, A. Baveling, C. Droste, M. Fechner, E. Haugland, M. Karlsen, M. Liane, S.O. Ryman, T.H. Vee, E. Wedershoven, and F. Øvstetun, "HAL4e – Hydro's New Generation Cell Technology", Light Metals 2009, pp. 371/75.
9. K. Grjotheim and H. Kvande, Introduction to Aluminium Electrolysis, 2nd Edition, Aluminium-Verlag GmbH, Düsseldorf, 1993.
10. J. Hives, J. Thonstad, Å. Sterten, and P. Fellner, "Electrical Conductivity of Molten Cryolite-Based Mixtures Obtained with a Tube-Type Cell Made of Pyrolytic Boron Nitride", Light Metals 1994, pp. 187/94.
11. R. Ødegård, A. Solheim, and K. Thovsen, "Current Pickup and Temperature Distribution in Newly Set Prebaked Hall-Héroult Anodes", Light Metals 1992, pp.457/63.
12. J. Thonstad, NTNU, personal communication (1992).
13. J. Thonstad, S. Rolseth, and R. Keller, "On the Mechanism behind Low Voltage PFC Emissions", Light Metals 2013, pp. 883/85.